APL Materials

In situ investigation of light soaking in organolead halide perovskite films

Cite as: APL Mater. **7**, 041114 (2019); https://doi.org/10.1063/1.5086125
Submitted: 18 December 2018 . Accepted: 13 March 2019 . Published Online: 16 April 2019

Yu Zhong, Carlos Andres Melo Luna, Richard Hildner, Cheng Li, and Sven Huettner

In situ investigation of light soaking in organolead halide perovskite films

Cite as: APL Mater. 7, 041114 (2019); doi: 10.1063/1.5086125
Submitted: 18 December 2018 • Accepted: 13 March 2019 •
Published Online: 16 April 2019 • Corrected: 29 May 2019

Yu Zhong,[1] Carlos Andres Melo Luna,[2,3] Richard Hildner,[2,a)] Cheng Li,[1,b),c)] and Sven Huettner[1,b)]

AFFILIATIONS

[1]Department of Chemistry, University of Bayreuth, Bayreuth 95447, Germany
[2]Spectroscopy of Soft Matter and Bayreuth Institute of Macromolecular Research, University of Bayreuth, Bayreuth 95447, Germany
[3]Centre for Bioinformatics and Photonics—CIBioFi, Universidad del Valle, 760032 Cali, Colombia

Note: This paper is part of the special topic on Perovskite Semiconductors for Next Generation Optoelectronic Applications.
[a)]**Current address:** Zernike Institute for Advanced Materials, University of Groningen, 9747 AG Groningen, The Netherlands.
[b)]**Authors to whom correspondence should be addressed:** cheng.li@uni-bayreuth.de and sven.huettner@uni-bayreuth.de
[c)]**Current address:** School of Electronic Science and Engineering, Xiamen University, Xiamen, 361005, China.

ABSTRACT

Organolead halide perovskite solar cells (PSCs) have generated extensive attention recently with power conversion efficiency (PCE) exceeding 23%. However, these PSCs exhibit photoinduced instability in the course of their current-voltage measurements. In this work, we study the light-induced behavior in $CH_3NH_3PbI_{3-x}Cl_x$ films *in situ*, by employing wide-field photoluminescence (PL) microscopy to obtain both the spatially and temporally resolved PL images simultaneously. Along with the increase in the PL intensity under continuous illumination, some areas render PL inactive. By characterizing the excitation energy dependent long-time PL decay behavior, we suggest that the PL quenching can be ascribed to a localized accumulation of iodide ions driven by the optical field. This ion localization leads to an enhancement of non-radiative recombination. The appearance of the PL inactive areas in the perovskite film impedes its photovoltaic device performance approaching the theoretical maximum PCE. Therefore, the herein presented real-time investigation of the light soaking of perovskite films is a versatile and adaptable method providing more details to improve the performance of PSCs.

Organolead halide perovskites [e.g., $CH_3NH_3PbX_3$ (X = I, Cl, Br)] have received intensive attention since 2012,[1,2] as they offer a new class of photovoltaic materials for low-cost and high-efficiency solar cells. Experiments toward a better understanding of their properties and fabrication processes have extensively been carried out, ranging from fundamental studies to device applications and long-term stability tests.[3–5] To minimize the degradation of the perovskite materials, scientists have made improvements on film quality and device stability, by controlling crystalline grain growth,[6,7] developing quasi-2D structures,[8,9] or incorporating different cations.[10,11] However, the detailed mechanism on optical/electrical induced degradation is still not fully elucidated.

Photoluminescence (PL), i.e., the radiative recombination process after optical excitation, has been demonstrated to give a strong correlation with film quality and device performance. The PL decay can demonstrate the charge carrier life time,[12,13] the spatial distribution of defect density, and the charge carrier recombination.[14,15] For instance, in the vicinity of perovskite grain boundaries, more defects are prevalent, resulting in non-radiative decay and a lower PL intensity.[16] Any non-radiative recombination would impair the carrier density buildup, preventing the photovoltaic device from approaching the theoretical Shockley-Queisser efficiency limit, i.e., the maximum theoretically achievable power conversion efficiency (PCE).[17]

The light soaking behavior of perovskite films is crucial for long-term stability of devices. It is reported that within light-soaking, the performance of perovskite solar cells (PSCs) improves.[18,19] However, under long-time illumination, perovskite films may also undergo at first reversible transformation[20,21] and then irreversible degradation.[22,23] These reversible transformations can be attributed to the formation of light-activated trap states[20] or photo-induced halide ion segregation.[21] In this work, we focus on the reversible

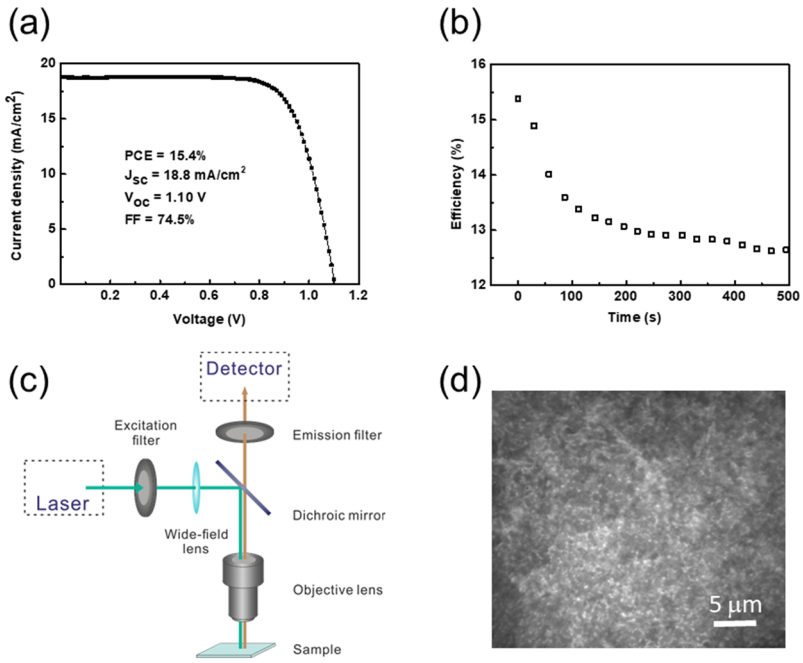

FIG. 1. (a) *J-V* curve of a PSC with the structure FTO/compact TiO_2/$CH_3NH_3PbI_{3-x}Cl_x$/Spiro-OMeTAD/Au. (b) The PCE decay of a planar PSC under continuous illumination (AM 1.5G) in nitrogen atmosphere with the scan rate of 0.8 V/s. (c) Schematic diagram of a wide-field PL microscope. (d) Wide-field PL image of a perovskite film using an exposure time of 50 ms and an excitation intensity of 40 mW/cm^2 at 532 nm wavelength.

changes in perovskite films. With a temporally and spatially resolved PL imaging method,[24] the presence of PL inactive areas on a micrometer scale was detected during light soaking, which should result from halide ion accumulation. By varying the laser intensity, the PL decay dynamics were studied.

Planar PSCs based on $CH_3NH_3PbI_{3-x}Cl_x$ were fabricated, with the highest PCE of 15.4% [current density-voltage (*J-V*) curve shown in Fig. 1(a)]. The device structure of these PSCs is shown in Fig. S3 of the supplementary material. We characterized the time dependent PCE of a solar cell device under continuous illumination (standard AM 1.5G illumination of 100 mW/cm^2) in nitrogen atmosphere. It was scanned from positive voltage to negative, noted as reverse scan. The PCE decreases to 12.6% within 500 s, as shown in Fig. 1(b). For comparison, we measured the PCE of a PSC without continuous illumination and the PCE showed a slight decrease. Already after 30 s of continuous light soaking, the PCE yielded a clear reduction for the herein used material system [illustrated in Fig. S5(a) of the supplementary material]. This suggests that this PCE decay is ascribed to the constant illumination rather than the electrical scanning. On the other hand, this light-induced PCE decay can be recovered in dark, as demonstrated in Fig. S5(b) of the supplementary material.

A thorough J-V characterization is presented in Fig. S4 of the supplementary material. With different scan rates and scan directions, the performance of a PSC varies. This is the hysteresis behavior discussed in many papers.[25–28] The relationship between the hysteresis and ion migration has been comprehensively reported.[26,28] Our PSC yields a distinct hysteresis behavior, which reveals that ion migration exists in this perovskite material. With continuous illumination, the hysteresis behavior of the PSC decreases (shown in Fig. S4-2 of the supplementary material). The PCE in forward scan increases (from negative voltage to positive) and in reverse scan decreases. It indicates the halide ion redistribution in perovskite.

The changes in short circuit current density (J_{sc}), open circuit voltage (V_{oc}), and fill factor (FF) under illumination are shown in Fig. S3 of the supplementary material. There is an obvious reduction of V_{oc}, while J_{sc} keeps nearly constant. For comparison, as shown in Fig. S5(a) of the supplementary material, a distinct V_{oc} decays with 30 s of illumination. In most cases, one dominant reason of the deterioration of a solar cell V_{oc} is the poor external luminescence efficiency.[15] The lower external luminescence reveals that some photons are wasted in nonradiative recombination or parasitic optical absorption.[17,29] For a working PSC, the decrease in external luminescence can result from the accumulation of ions on the interface.[30] Our measurements indicate that besides the bias-driven ion effect, the illumination is another factor of luminescence decay. Tracking the long-time PL behavior with a wide-field PL microscope is a good way to locally study the carrier recombination in perovskite films. Thus, we employed this method to investigate the light-induced long-term decay effect. The detailed description of this technique has been reported elsewhere.[31,32] Briefly, a wide field PL microscope equipped with an oil-immersion objective with a 100× magnification, a 532 nm laser for excitation, and a fast charge-coupled device (CCD) camera was employed to track the time dependent fluorescence as shown in Fig. 1(c). Note that the perovskite films were covered with polymethyl methacrylate (PMMA) to be protected from ambient air.[33] To illuminate a large area (diameter ~60 μm) of the film homogeneously, we additionally inserted a wide-field lens in the excitation beam path. Rather than small areas characterized by classical confocal microscopy,[34] this allows us to characterize the temporal and spatial evolutions of the PL intensity in a larger area with time-resolution as short as 50 ms and a spatial resolution of about 300 nm. Figure 1(d) shows a PL image of a $CH_3NH_3PbI_{3-x}Cl_x$ perovskite film. It displays densely packed grains with a few pinholes, which is consistent with the image taken by a scanning electron

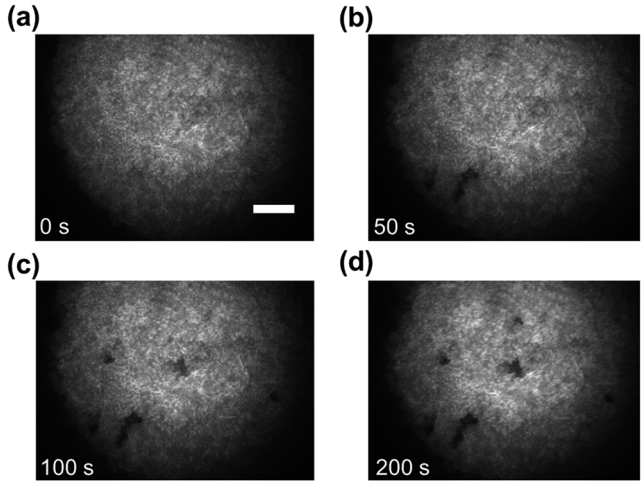

FIG. 2. [(a)–(d)] Temporal evolution of a PL image on the surface of perovskite under light illumination of 40 mW/cm^2 at 532 nm wavelength. The scale bar is 10 μm, and the integration time is 50 ms. The corresponding video is shown in S10 of the supplementary material.

microscope (SEM) (Fig. S6-1 of the supplementary material). Due to the limited resolution of optical microscopy, grains with size smaller than 300 nm cannot be distinguished anymore. Correlated SEM and PL images at one spot are presented in Fig. S6-2 of the supplementary material and we can observe the PL emission from each crystal grain. Additionally, the morphology of this perovskite film is similar to the perovskite film spin coated on the TiO_2 layer (Fig. S6-3 of the supplementary material). Thus, it is acceptable to use this perovskite film in order to study the light-soaking behavior.

Figure 2 shows a series of PL images of the perovskite surface under continuous light illumination (532 nm, 40 mW/cm^2). Beside a PL intensity increase of the whole film, certain dark regions are observed. The first PL dark region, which is in the left bottom part of the image [see Fig. 2(b)], appeared within 10 s. This indicates that charge carrier recombination in these areas transforms from radiative to non-radiative. With longer illumination time, the number of dark areas increases. The overall PL evolution is shown in the supplementary material, S10 Video. This phenomenon is described as the appearance of PL inactive areas or PL quenching in this work. We analyze the temporal PL intensity of one PL inactive area and find that the PL intensity yields an enhancement within the first 45 s and then it decreases, as illustrated in Fig. 3(a). Except for the PL inactive areas, the PL intensity of the other part increases, as shown in Fig. 3(b). This PL increase of the perovskite film under illumination has been reported,[35,36,32] arising from traps filled,[37] or defect annihilation during light illumination.[38,39]

The phenomenon that the PL intensity of the perovskite film decreases after a PL enhancement has been discussed recently. Gottesman *et al.* observed that the PL of a $CH_3NH_3PbI_3$ film gradually decreased by ~40% under 1 h illumination.[40] Juan *et al.* found a PL decrease following a PL enhancement of the bulk perovskite film both in air and in nitrogen.[41] The V_{oc} of PSCs is related to the PL intensity because the PL lowering indicates that the generation of trap states reduces the quasi-Fermi-level for the electrons[42] and consequently leads to a decrease in the V_{oc}.[18,19] In Fig. S3(c) of the supplementary material, the V_{oc} of a PSC shows an obvious decrease within the first 100 s and resembles the time when the PL dark areas show up.

In order to elucidate the origin of this PL quenching phenomenon, first, we need to assess whether it is caused by chemical

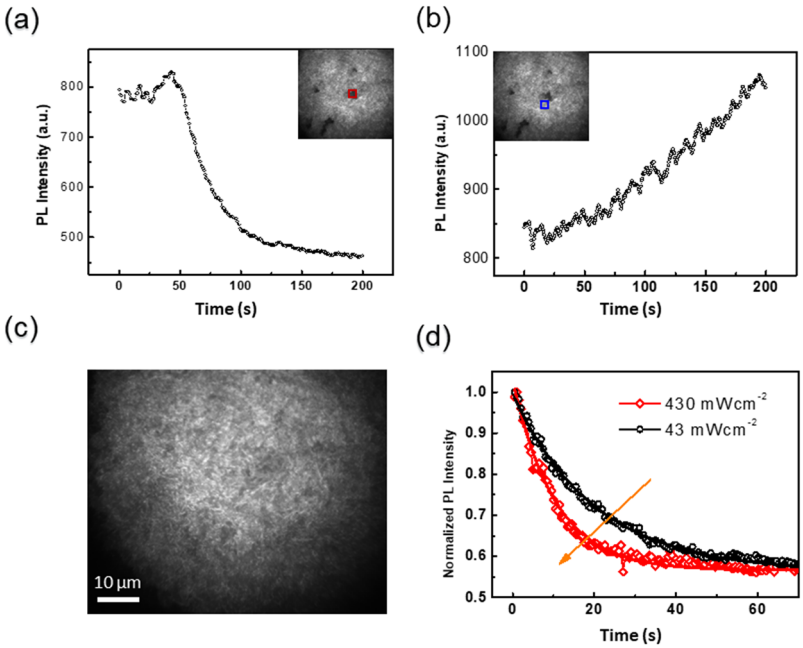

FIG. 3. [(a) and (b)] The average PL intensity of two local regions in the series of PL images in Fig. 2 as a function of time. The two insets in (a) and (b) demonstrate the location of these two regions. The time dependent PL intensity of the two rectangle areas was displayed. (c) The PL image of the perovskite film, which was observed in Fig. 2, was kept in dark after continuous illumination and was measured again here after its recovery. (d) Normalized temporal evolution of a PL intensity quenching area under continuous illumination of different intensities. The red and black solid lines are the fitting lines based on single exponential functions. The decay time is estimated 15.1 s and 29.4 s for illumination intensity 430 mW/cm^2 and 43 mW/cm^2, respectively.

degradation of perovskite. After laser illumination, the perovskite film was kept in dark for several minutes and its PL image was obtained in Fig. 3(c). We found that the PL inactive or PL quenching areas in the film reverted to their PL active state, i.e., showing radiative recombination again. This indicates that this process is reversible, originating from ionic movement,[32,20] reversible structural transformation,[40,43] or surface charge trapping/detrapping[44,45] rather than an irreversible chemical degradation, e.g., long-term decomposition of perovskite[46,22] or gas release of CH_3NH_3I after long-term electrical biasing.[47,48] Furthermore, it seems not to originate from the reversible perovskite hydration process. When perovskite hydrates form, the PL intensity at boundaries tends to increase as shown in Fig. S9 of the supplementary material. The reason is that perovskite hydrates first form at the grain interfaces and these hydrates will impede carrier transport along different grains.[49,50] As a result, the recombination at the grain interfaces is enhanced.[49] This is different from the results observed in Fig. 2.

To investigate the mechanism of the PL quenching, the temporal evolution of the PL signal on individual grains under different illumination intensities is studied. As shown in Fig. 3(a), the PL intensity in the dark areas decays under continuous light soaking. Taking into account three individual domains observed under different excitation intensities, we obtain that the long-term decay time is 25 ± 9 s for 43 mW/cm^2 and 13 ± 6 s for 430 mW/cm^2, following single exponential functions. The PL intensity of these grains decays faster under high illumination (430 mW/cm^2) intensity than under low intensity (43 mW/cm^2), consistent with the observation by Chen *et al.*[34] The time scale of the PL decay is ~10 s, which is in the same time scale of halide ion migration in the perovskite film.[26,34,51] Meanwhile, our J-V measurements on PSCs yield hysteretic behavior, suggesting the possible halide ion (i.e., vacancy) migration. We can therefore associate this PL quenching behavior with the migration and accumulation of ions.

Several studies have proved the halide ion migration in the organolead perovskite film. By combination of time-of-flight secondary-ion-mass spectrometry (ToF-SIMS) and PL microscopy, deQuilettes *et al.* detected the iodide element signal through a depth profile at the illuminated region and showed the iodide redistribution with the optical field.[38] In addition, the results of scanning Kelvin probe microscopy (SKPM) demonstrated a surface potential shift of the perovskite layer under illumination,[52–54] which can drive the mobile ions. The activation energy of the iodide migration in the perovskite polycrystalline thin film has been estimated between ~0.1 eV and ~0.6 eV.[51,55,56] Xing *et al.*[57] found the reduction of the activation energy of mobile ions under illumination. Very recently, Li *et al.* pointed out the role of iodide vacancies as the main migrating species respective to iodide ions.[58] Therefore, we reiterate that the light-induced electrical field in the film can promote the iodide ions/vacancies to migrate.

We propose that the origin of the PL inactive areas in Fig. 2 is the redistribution and localization of halide ions. Both Hoke *et al.*[59] and Yoon *et al.*[21] also successfully tracked the formation of I-rich and Br-rich domains in $MAPb(Br_xI_{1-x})_3$ films, which is induced from the halide ion movement under illumination. As reported, halide ions in perovskites possess a relatively low activation energy, compared to other ions.[56] Therefore, with light-soaking, halide ions tend to migrate more readily in the perovskite film and localize at grain boundaries or some defective grains. That may happen, when halide ions are immobilized at grains with a high defect density potentially allowing the formation of further interstitial defects that render non-radiative recombination centers.[60,61] Another possibility is the segregation of halide ions at grain boundaries.[62] In these segregated domains, the recombination changes from radiative to non-radiative.

As briefly mentioned above, interstitial defects indeed may play a significant role in quenched photoluminescence, creating deep trap states and acting as non-radiative recombination centers.[20,63] It is worth mentioning that calculations attribute, among native point defects, only iodine interstitials to form deep carrier traps and non-radiative recombination centers, whereas all vacancies, cation interstitials, and some antisite defects create only shallow levels.[60,61] The origin of point defects shall be found in Frenkel defects, forming a vacancy and an interstitial, which have been reported to be abundant in MAPI films.[64] The much higher diffusion constant of vacancies compared to interstitials leaves behind interstitials as non-radiative recombination centers.[65,60,66] In a similar context, it has been reported that a bias voltage is applied on a perovskite film with laterally configured electrodes, facilitating an increasingly PL quenched region starting from the positive electrode. This is a consequence of iodide vacancies migrating towards the negative electrode,[32,34] changing the effective electron-hole concentration[58] and leaving a larger number of interstitials behind acting as non-radiative quenching sites.

We found that two main factors for the appearance of these PL inactive areas are the optical intensity gradient of the light source and the film quality. Another PL microscope with a white light-emitting diode (LED) was used to observe this light-soaking effect. In the center of the illuminated area, few PL dark areas were detected. Most PL dark areas are present at the edge of the exposed area (shown in Fig. 4). This is exactly correlated with the light source beam profile as shown in Fig. S8(b) of the supplementary material with a strong intensity gradient right at the edge of the illuminated

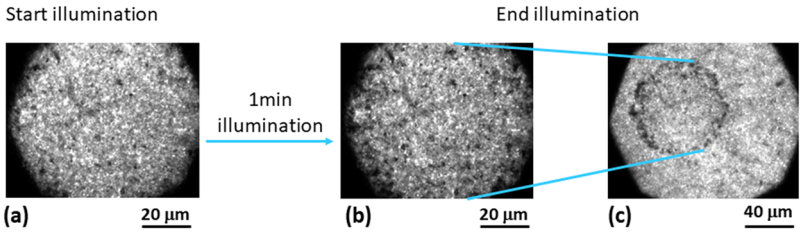

FIG. 4. Perovskite film was observed at the beginning (a) and the end [(b) and (c)] of illumination. The light source is a white LED with a short pass filter of 440 nm. Its beam profile is displayed in Fig. S8(b) of the supplementary material. The difference between (b) and (c) is that a different object lens was used. Only the region in (b) was under illumination and the other regions were in dark. The guideline means that the region between the guidelines in (c) is the same region in (b).

area. It reveals that the horizontal optical intensity gradient is crucial for driving mobile ions and ion-aggregated PL quenching behavior. We also notice that an old film shows more PL inactive areas than a fresh film. It is ascribed to the degradation of perovskite and more defects or mobile ions in the old film. Thus, the film quality and the presence of surface defects is an important factor. To check this, we employed this experiment on a perovskite film with PCBM molecules, which have been shown to passivate surface/grain boundary defects.[67,68] This passivated perovskite film exhibits little difference in PL images before and after illumination, even at high excitation intensities and gradients [as displayed in Figs. S7(e)–S7(j) of the supplementary material]. It needs to be noted that not only the passivated defects in perovskite films but also the weakened light-induced field by PCBM contributes to this phenomenon.

By combining the above analysis, the proposed mechanism of PL quenching phenomenon is illustrated in Fig. 5. Before illumination, the iodide ions are uniformly distributed in the perovskite film, as shown in Fig. 5(a). Under illumination, the optical field decreases with penetration depth and is laterally limited by

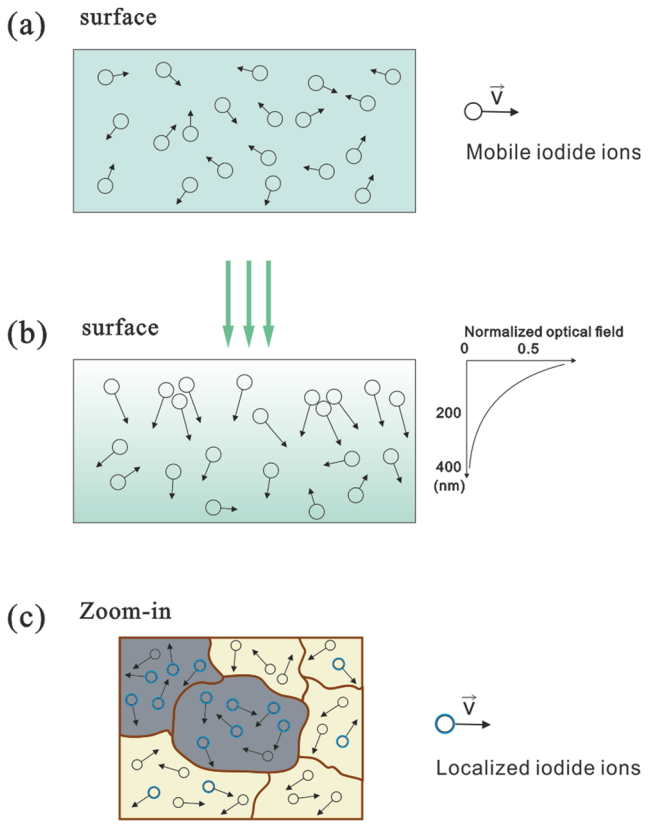

FIG. 5. The schematic of light-induced PL inactive areas: (a) The perovskite film without illumination. The iodide ions uniformly distribute through the film and have limited mobility. (b) Under illumination, the iodide ions get more energy and higher mobility. They can drift with the local optical field. (c) The mobile iodide ions can drift within a certain distance. When the local region has more defects, the ions will move there. The accumulation of iodide ions leads to non-radiative recombination. The arrow in the figure is for the possible moving direction of iodide ions and the magnitude of the arrow is for the mobility.

its spot size, giving rise to gradients in the diffusion constants of ion field both vertically and horizontally, which redistributes iodide ions. During the migration process, regions with higher density of defects can result in the localization of ions.[61,69,70] Different effects can lead to non-radiative recombination: Charge accumulation at surface and grain boundaries enhance Auger-type non-radiative recombination, which is predominantly seen in nanoparticles.[69] Iodide interstitials, in particular, have been pointed out to create deep level defects, resulting in non-radiative recombination centers.[61] Also, the change in the effective hole concentration towards more intrinsic may reduce the PL quantum yield.[58] Given the fact that the herein observed effects are rather inhomogeneously distributed and become stronger with lower quality of films, the assumption is that the creation of defect sites (i.e., interstitials) is caused by the local sample inhomogeneities and the accumulation of iodide ions at defective grains as illustrated in Fig. 5(c). The migration pathway can be through the iodine interstitial sites.[71] When the illumination intensity increases, the activation energy of halide ions decreases,[57,72] leading to a faster migration and hence an enhanced possible trapping and accumulation of ions at defect sites resulting in a faster PL decay of these regions. This explains the observation in Fig. 4(c) that more PL inactive areas appear at the edge beyond the illuminated area, where the iodide ions are driven out. Once they reach the non-illuminated area, their mobility will decrease and they will be almost immobile there, thus leading to a certain localization of redistributed iodide ions. We speculate that this additionally increases the chance for the formation of interstitial defects taking into account their low formation energy,[39,73] rendering non-radiative recombination centers.

The appearance of dark PL-inactive areas in perovskite films under illumination reveals that the migration and accumulation of halide ions has a negative effect on the stable output of perovskite photovoltaics. Thus, suppressing the halide ion migration in the perovskite films is one of the key issues to further improve the performance and stability of photovoltaic devices. Controlling the crystal quality and size can be an effective way,[74] as most of the mobile ions originate from defects at the grain boundaries/surface.[36,70,75] Another choice is passivating the defects with external particles, such as PCBM[68] or K^+.[11] Meanwhile, the intensity distribution of the light source should be an issue for the stable output of PSCs.

In summary, wide-field PL microscopy is demonstrated as a simple and versatile method in characterizing the quality and stability of perovskite films. We employed wide-field PL microscopy to *in situ* investigate the PL changes of a perovskite film with light soaking on time scales of seconds. Besides the PL enhancement, some areas in the film yield a PL quenching. This PL quenching behavior plays an important role in PSCs because non-radiative recombination prevents PCEs from approaching the Shockley-Queisser efficiency limit. By characterizing the intensity dependent PL long-time decay process, we observe that the migration and localization of iodide ions in the perovskite film within an optical field gradient contribute to this non-radiative recombination. It is the first time to visually observe the accumulation of iodide ions during light soaking inducing non-radiative recombination. This either occurs at defective sites that are prone to accumulate and trap ions or at the gradient between the illuminated and non-illuminated areas.

See supplementary material for the sample preparation method, characterization details, the change in V_{oc}, J_{sc}, and FF with light soaking, the observation of $CH_3NH_3PbI_{3-x}Cl_x$ film with AFM, SEM, and PL microscopy, and the beam profile of light source.

Financial support by the Bavarian State Ministry of Science, Research and the Arts for the Collaborative Research Network "Solar Technologies go Hybrid" and Federal Ministry of Education as well as the German Research Foundation (DFG) is gratefully acknowledged. Richard Hildner and Carlos Andres Melo Luna acknowledge additional funding from DFG - GRK1640. Yu Zhong acknowledges funding from the China Scholarship Council. Carlos Andres Melo Luna acknowledges funding from the Colombian Science, Technology and Innovation Fund-General Royalties System (Fondo CTeI-Sistema General de Regalías, Contract No. BPIN 2013000100007) and CIBioFi. We thank Jürgen Köhler and Kevin Wilma for experimental support. This open access publication was funded through the Open Access Publishing programme of the DFG and University of Bayreuth.

REFERENCES

[1] W. S. Yang, J. H. Noh, N. J. Jeon, Y. C. Kim, S. Ryu, J. Seo, and S. I. Seok, Science **348**, 1234 (2015).
[2] H.-S. Kim, C.-R. Lee, J.-H. Im, K.-B. Lee, T. Moehl, A. Marchioro, S.-J. Moon, R. Humphry-Baker, J.-H. Yum, J. E. Moser, M. Grätzel, and N.-G. Park, Sci. Rep. **2**, 591 (2012).
[3] S. D. Stranks, G. E. Eperon, G. Grancini, C. Menelaou, M. J. P. Alcocer, T. Leijtens, L. M. Herz, A. Petrozza, and H. J. Snaith, Science **342**, 341 (2013).
[4] G. Xing, N. Mathews, S. Sun, S. S. Lim, Y. M. Lam, M. Gratzel, S. Mhaisalkar, and T. C. Sum, Science **342**, 344 (2013).
[5] F. Panzer, C. Li, T. Meier, A. Köhler, and S. Huettner, Adv. Energy Mater. **7**, 1700286 (2017).
[6] X. Li, D. Bi, C. Yi, J.-D. Décoppet, J. Luo, S. M. Zakeeruddin, A. Hagfeldt, and M. Grätzel, Science **353**, 58 (2016).
[7] N.-G. Park, M. Grätzel, T. Miyasaka, K. Zhu, and K. Emery, Nat. Energy **1**, 16152 (2016).
[8] Z. Wang, Q. Lin, F. P. Chmiel, N. Sakai, L. M. Herz, and H. J. Snaith, Nat. Energy **2**, 17135 (2017).
[9] G. Grancini, C. Roldán-Carmona, I. Zimmermann, E. Mosconi, X. Lee, D. Martineau, S. Narbey, F. Oswald, F. De Angelis, M. Graetzel, and M. K. Nazeeruddin, Nat. Commun. **8**, 15684 (2017).
[10] M. Saliba, T. Matsui, K. Domanski, J.-Y. Seo, A. Ummadisingu, S. M. Zakeeruddin, J.-P. Correa-Baena, W. R. Tress, A. Abate, A. Hagfeldt, and M. Gratzel, Science **354**, 206 (2016).
[11] D.-Y. Son, S.-G. Kim, J.-Y. Seo, S.-H. Lee, H. Shin, D. Lee, and N.-G. Park, J. Am. Chem. Soc. **140**, 1358 (2018).
[12] J. A. Giesecke, M. C. Schubert, B. Michl, F. Schindler, and W. Warta, Sol. Energy Mater. Sol. Cells **95**, 1011 (2011).
[13] Z. Hameiri, A. Mahboubi Soufiani, M. K. Juhl, L. Jiang, F. Huang, Y.-B. Cheng, H. Kampwerth, J. W. Weber, M. A. Green, and T. Trupke, Prog. Photovoltaics: Res. Appl. **23**, 1697 (2015).
[14] K. Zheng, K. Žídek, M. Abdellah, M. E. Messing, M. J. Al-Marri, and T. Pullerits, J. Phys. Chem. C **120**, 3077 (2016).
[15] W. Tress, Adv. Energy Mater. **7**, 1602358 (2017).
[16] D. W. de Quilettes, S. M. Vorpahl, S. D. Stranks, H. Nagaoka, G. E. Eperon, M. E. Ziffer, H. J. Snaith, and D. S. Ginger, Science **348**, 683 (2015).
[17] O. D. Miller, E. Yablonovitch, and S. R. Kurtz, IEEE J. Photovoltaics **2**, 303 (2012).
[18] Y. Deng, Z. Xiao, and J. Huang, Adv. Energy Mater. **5**, 1500721 (2015).
[19] C. Zhao, B. Chen, X. Qiao, L. Luan, K. Lu, and B. Hu, Adv. Energy Mater. **5**, 1500279 (2015).
[20] W. Nie, J.-C. Blancon, A. J. Neukirch, K. Appavoo, H. Tsai, M. Chhowalla, M. A. Alam, M. Y. Sfeir, C. Katan, J. Even, S. Tretiak, J. J. Crochet, G. Gupta, and A. D. Mohite, Nat. Commun. **7**, 11574 (2016).
[21] S. J. Yoon, S. Draguta, J. S. Manser, O. Sharia, W. F. Schneider, M. Kuno, and P. V. Kamat, ACS Energy Lett. **1**, 290 (2016).
[22] W. Huang, S. J. Yoon, and P. Sapkota, ACS Appl. Energy Mater. **1**, 2859 (2018).
[23] R. P. Xu, Y. Q. Li, T. Y. Jin, Y. Q. Liu, Q. Y. Bao, C. O'Carroll, and J. X. Tang, ACS Appl. Mater. Interfaces **10**, 6737 (2018).
[24] C. A. Combs, Curr. Protoc. Neurosci. **50**, 2.1.1 (2010).
[25] S. N. Habisreutinger, N. K. Noel, and H. J. Snaith, ACS Energy Lett. **3**, 2472 (2018).
[26] C. Li, S. Tscheuschner, F. Paulus, P. E. Hopkinson, J. Kießling, A. Köhler, Y. Vaynzof, and S. Huettner, Adv. Mater. **28**, 2446 (2016).
[27] B. Chen, M. Yang, X. Zheng, C. Wu, W. Li, Y. Yan, J. Bisquert, G. Garcia-Belmonte, K. Zhu, and S. Priya, J. Phys. Chem. Lett. **6**, 4693 (2015).
[28] D. A. Jacobs, Y. Wu, H. Shen, C. Barugkin, F. J. Beck, T. P. White, K. Weber, and K. R. Catchpole, Phys. Chem. Chem. Phys. **19**, 3094 (2017).
[29] R. T. Ross, J. Chem. Phys. **46**, 4590 (1967).
[30] A. M. Soufiani, Z. Hameiri, S. Meyer, S. Lim, M. J. Y. Tayebjee, J. S. Yun, A. Ho-Baillie, G. J. Conibeer, L. Spiccia, and M. A. Green, Adv. Energy Mater. **7**, 1602111 (2017).
[31] A. T. Haedler, K. Kreger, A. Issac, B. Wittmann, M. Kivala, N. Hammer, J. Kohler, H.-W. Schmidt, and R. Hildner, Nature **523**, 196 (2015).
[32] C. Li, A. Guerrero, Y. Zhong, A. Gräser, C. A. M. Luna, J. Köhler, J. Bisquert, R. Hildner, and S. Huettner, Small **13**, 1701711 (2017).
[33] H. Yu, F. Wang, F. Xie, W. Li, J. Chen, and N. Zhao, Adv. Funct. Mater. **24**, 7102 (2014).
[34] S. Chen, X. Wen, R. Sheng, S. Huang, X. Deng, M. A. Green, and A. Ho-Baillie, ACS Appl. Mater. Interfaces **8**, 5351 (2016).
[35] C. Li, Y. Zhong, C. Luna, T. Unger, K. Deichsel, A. Gräser, J. Köhler, A. Köhler, R. Hildner, and S. Huettner, Molecules **21**, 1081 (2016).
[36] Y. Tian, A. Merdasa, E. Unger, M. Abdellah, K. Zheng, S. McKibbin, A. Mikkelsen, T. Pullerits, A. Yartsev, V. Sundström, and I. G. Scheblykin, J. Phys. Chem. Lett. **6**, 4171 (2015).
[37] S. Chen, X. Wen, S. Huang, F. Huang, Y.-B. Cheng, M. Green, and A. Ho-Baillie, Sol. RRL **1**, 1600001 (2017).
[38] D. W. deQuilettes, W. Zhang, V. M. Burlakov, D. J. Graham, T. Leijtens, A. Osherov, V. Bulović, H. J. Snaith, D. S. Ginger, and S. D. Stranks, Nat. Commun. **7**, 11683 (2016).
[39] E. Mosconi, D. Meggiolaro, H. J. Snaith, S. D. Stranks, and F. De Angelis, Energy Environ. Sci. **9**, 3180 (2016).
[40] R. Gottesman, L. Gouda, B. S. Kalanoor, E. Haltzi, S. Tirosh, E. Rosh-Hodesh, Y. Tischler, A. Zaban, C. Quarti, E. Mosconi, and F. De Angelis, J. Phys. Chem. Lett. **6**, 2332 (2015).
[41] J. F. Galisteo-López, M. Anaya, M. E. Calvo, and H. Míguez, J. Phys. Chem. Lett. **6**, 2200 (2015).
[42] S. D. Stranks, V. M. Burlakov, T. Leijtens, J. M. Ball, A. Goriely, and H. J. Snaith, Phys. Rev. Appl. **2**, 034007 (2014).
[43] R. Gottesman and A. Zaban, Acc. Chem. Res. **49**, 320 (2016).
[44] T. Tachikawa, I. Karimata, and Y. Kobori, J. Phys. Chem. Lett. **6**, 3195 (2015).
[45] H. Yuan, E. Debroye, G. Caliandro, K. P. F. Janssen, J. van Loon, C. E. A. Kirschhock, J. A. Martens, J. Hofkens, and M. B. J. Roeffaers, ACS Omega **1**, 148 (2016).
[46] G. Niu, W. Li, F. Meng, L. Wang, H. Dong, and Y. Qiu, J. Mater. Chem. A **2**, 705 (2014).
[47] X. Deng, X. Wen, J. Lau, T. Young, J. Yun, M. Green, S. Huang, and A. W. Y. Ho-Baillie, J. Mater. Chem. C **4**, 9060 (2016).
[48] H. Yuan, E. Debroye, K. Janssen, H. Naiki, C. Steuwe, G. Lu, M. Moris, E. Orgiu, H. Uji-i, F. De Schryver, P. Samorì, J. Hofkens, and M. Roeffaers, J. Phys. Chem. Lett. **7**, 561 (2016).

[49]A. M. A. Leguy, Y. Hu, M. Campoy-Quiles, M. I. Alonso, O. J. Weber, P. Azarhoosh, M. Van Schilfgaarde, M. T. Weller, T. Bein, J. Nelson, P. Docampo, and P. R. F. Barnes, Chem. Mater. **27**, 3397 (2015).
[50]Z. Song, A. Abate, S. C. Watthage, G. K. Liyanage, A. B. Phillips, U. Steiner, M. Graetzel, and M. J. Heben, Adv. Energy Mater. **6**, 1600846 (2016).
[51]C. Eames, J. M. Frost, P. R. F. Barnes, B. C. O'Regan, A. Walsh, and M. S. Islam, Nat. Commun. **6**, 7497 (2015).
[52]J. R. Harwell, T. K. Baikie, I. D. Baikie, J. L. Payne, C. Ni, J. T. S. Irvine, G. A. Turnbull, and I. D. W. Samuel, Phys. Chem. Chem. Phys. **18**, 19738 (2016).
[53]V. W. Bergmann, S. A. L. Weber, F. Javier Ramos, M. K. Nazeeruddin, M. Grätzel, D. Li, A. L. Domanski, I. Lieberwirth, S. Ahmad, and R. Berger, Nat. Commun. **5**, 5001 (2014).
[54]V. W. Bergmann, Y. Guo, H. Tanaka, I. M. Hermes, D. Li, A. Klasen, S. A. Bretschneider, E. Nakamura, R. Berger, and S. A. L. Weber, ACS Appl. Mater. Interfaces **8**, 19402 (2016).
[55]J. M. Azpiroz, E. Mosconi, J. Bisquert, and F. De Angelis, Energy Environ. Sci. **8**, 2118 (2015).
[56]C. Li, A. Guerrero, Y. Zhong, and S. Huettner, J. Phys.: Condens. Matter **29**, 193001 (2017).
[57]J. Xing, Q. Wang, Q. Dong, Y. Yuan, Y. Fang, and J. Huang, Phys. Chem. Chem. Phys. **18**, 30484 (2016).
[58]C. Li, A. Guerrero, S. Huettner, and J. Bisquert, Nat. Commun. **9**, 5113 (2018).
[59]E. T. Hoke, D. J. Slotcavage, E. R. Dohner, A. R. Bowring, H. I. Karunadasa, and M. D. McGehee, Chem. Sci. **6**, 613 (2015).
[60]M. H. Du, J. Phys. Chem. Lett. **6**, 1461 (2015).
[61]M. H. Du, J. Mater. Chem. A **2**, 9091 (2014).
[62]D. J. Slotcavage, H. I. Karunadasa, and M. D. McGehee, ACS Energy Lett. **1**, 1199 (2016).
[63]D. Meggiolaro, S. G. Motti, E. Mosconi, A. J. Barker, J. Ball, C. Andrea Riccardo Perini, F. Deschler, A. Petrozza, and F. De Angelis, Energy Environ. Sci. **11**, 702 (2018).
[64]S. T. Birkhold, J. T. Precht, R. Giridharagopal, G. E. Eperon, L. Schmidt-Mende, and D. S. Ginger, J. Phys. Chem. C **122**, 12633 (2018).
[65]D. Meggiolaro, E. Mosconi, and F. De Angelis, ACS Energy Lett. **3**, 447 (2018).
[66]H. Shi and M. H. Du, Phys. Rev. B **90**, 174103 (2014).
[67]Y. Shao, Z. Xiao, C. Bi, Y. Yuan, and J. Huang, Nat. Commun. **5**, 5784 (2014).
[68]J. Xu, A. Buin, A. H. Ip, W. Li, O. Voznyy, R. Comin, M. Yuan, S. Jeon, Z. Ning, J. J. McDowell, P. Kanjanaboos, J.-P. Sun, X. Lan, L. N. Quan, D. H. Kim, I. G. Hill, P. Maksymovych, and E. H. Sargent, Nat. Commun. **6**, 7081 (2015).
[69]X. Wen, A. Ho-Baillie, S. Huang, R. Sheng, S. Chen, H. Ko, and M. A. Green, Nano Lett. **15**, 4644 (2015).
[70]Y. Yuan and J. Huang, Acc. Chem. Res. **49**(2), 286 (2016).
[71]J. L. Minns, P. Zajdel, D. Chernyshov, W. Van Beek, and M. A. Green, Nat. Commun. **8**, 15152 (2017).
[72]Y. C. Zhao, W. K. Zhou, X. Zhou, K. H. Liu, D. P. Yu, and Q. Zhao, Light: Sci. Appl. **6**, e16243 (2017).
[73]W. J. Yin, T. Shi, and Y. Yan, Appl. Phys. Lett. **104**, 063903 (2014).
[74]W. Nie, H. Tsai, R. Asadpour, A. J. Neukirch, G. Gupta, J. J. Crochet, M. Chhowalla, S. Tretiak, M. A. Alam, and H. Wang, Science **347**, 522 (2015).
[75]J. S. Yun, J. Seidel, J. Kim, A. M. Soufiani, S. Huang, J. Lau, N. J. Jeon, S. Il Seok, M. A. Green, and A. Ho-Baillie, Adv. Energy Mater. **6**, 1600330 (2016).